Role of van der Waals corrections for the PtX_2 (X = O, S, Se) compounds

Maurício J. Piotrowski*
Instituto de Física e Matemática, Universidade Federal de Pelotas, Caixa Postal 354, 96010-900, Pelotas, RS, Brazil and Instituto de Química de São Carlos, Universidade de São Paulo, Caixa Postal 780, 13560-970, São Carlos, SP, Brazil

Ricardo K. Nomiyama†
Escola de Engenharia de São Carlos, Universidade de São Paulo, Caixa Postal 359, 13566-590, São Carlos, SP, Brazil

Juarez L. F. Da Silva‡
Instituto de Química de São Carlos, Universidade de São Paulo, Caixa Postal 780, 13560-970, São Carlos, SP, Brazil
(Received 9 June 2013; published 15 August 2013)

Dispersion (van der Waals) forces play an important role in determining the structural properties of the systems where dispersion is crucial, for example, layerlike crystals (CdI_2 type). Thus, to contribute to the understanding of the role of van der Waals (vdW) corrections for the PtX_2 (X = O, S, Se) compounds, we report a density functional theory (DFT) investigation within nonlocal vdW corrections for the atomic structure and electronic properties of bulk PtX_2. From our calculations, we identified the lowest energy structures, $CaCl_2$ type for PtO_2 and CdI_2 type for both PtS_2 and $PtSe_2$, i.e., CdI_2 type is not the lowest energy structure for PtO_2. We reported the structural changes for higher energy PtX_2 systems and the changes in the stability order compared with plain DFT-PBE calculations. The structural changes induced by vdW corrections affects the electronic structure of the layered CdI_2-type structures (PtS_2 and $PtSe_2$), where a metallic behavior is obtained in contrast to PBE calculations, which yields an energy separation between the unoccupied and occupied states.

DOI: 10.1103/PhysRevB.88.075421 PACS number(s): 63.20.dk, 61.66.−f, 61.82.Ms

I. INTRODUCTION

There is a great interest in platinum dioxide (PtO_2) and dichalcogenides (PtS_2, $PtSe_2$) systems due to the wide range of promising applications in electrochemistry and catalysis.[1–4] For example, Sabourault *et al.*[1] reported that PtO_2 is a powerful hydrosilylation catalyst, while the CO oxidation on PtO_2 surfaces has been studied by Gong *et al.*[3] and Ackermann *et al.*[4] They observed a substantially higher catalytic activity than the bulk-terminated Pt surface (and other studied compounds). Dey *et al.*[2] suggested that platinum dichalcogenides are good catalysts for several reactions, e.g., hydrodesulfurization, hydrodenitrogenation, hydrogenation, and dehydrogenation reactions, etc. Furthermore, it has been reported that PtS_2 nanoclusters have promising band gap properties, constituting viable semiconductors to electronic applications.[5] Although several studies have been reported for those compounds (PtO_2, PtS_2, and $PtSe_2$), a basic understanding of the structure and electronic properties remains incomplete and further studies are highly desirable due to the wide importance of platinum dioxide and dichalcogenides systems.

Experimentally, several studies have indicated that platinum dioxide (PtO_2) adopts the layered CdI_2-type and distorted Rutile ($CaCl_2$-type) structures,[6–8] however, several experimental studies have identified only the Rutile-type structures.[9,10] Platinum disulfides (PtS_2) and diselenides ($PtSe_2$) crystallize in the layered CdI_2-type structure,[11,12] and there is no experimental observation of further crystal structures, which is in contrast with few crystal structures reported for PtO_2.[6–10] $CaCl_2$ type is an orthorhombic structure which consists of a slightly distorted variant of the tetragonal Rutile-type structure. The CdI_2-type structure presents a laminar crystal structure, where each PtX_2 layer is made up of edge-sharing octahedra, and the three-dimensional structure is obtained by stacking PtX_2 layers.

The interactions between the adjacent CdI_2 layers might be weak due to the large interlayer separation, e.g., c_0 = 4.8 Å for PtO_2,[6] and hence the asymptotic long range nonlocal van der Waals (vdW) interactions might play an important role.[13,14] Standard first-principles calculations based on density-functional theory (DFT), using local or semilocal exchange-correlation (xc) functionals, cannot provide a correct description of the nonlocal vdW interactions (dispersion forces). For example, several plain DFT studies of layered materials have overestimated the equilibrium interlayer distances.[15–20]

For PtO_2, contrary to experimental evidence, but in agreement with previous DFT calculations,[21,22] the CdI_2 structure is less stable than $CaCl_2$-type structure. The theoretical CdI_2 destabilization could be due to the underestimation of the interlayer binding energy by plain DFT. Thus, could an appropriate vdW treatment improve the description of the interlayer interaction in CdI_2 and, consequently, stabilize the CdI_2 structure? Furthermore, for PtS_2 and $PtSe_2$ systems, for which DFT calculations have reported the CdI_2 type as the lowest energy structure, a theoretical treatment considering the vdW interactions could improve the agreement of structural and electronic properties compared with experimental results?

To contribute to the solution of those open questions, we have performed a first-principles investigation of the atomic structures of the PtO_2, PtS_2, and $PtSe_2$ systems employing DFT within vdW corrections to the semilocal functionals. We found that vdW correction is fundamental to obtain a reliable description of the equilibrium volume of the CdI_2 structure, while the stability of the CdI_2 structure is decreased compared with the $CaCl_2$ structure for PtO_2.

II. THEORETICAL APPROACH AND COMPUTATIONAL DETAILS

Our calculations are based on the spin-polarized DFT within the generalized gradient approximation (GGA) proposed by Perdew, Burke, and Erzenhoff[24] (PBE), as implemented in the Vienna *ab initio* simulation package (VASP).[25,26] To provide a better description of the nonlocal vdW interactions, which has been known to play an important role in several systems, e.g., layered crystals,[27,28] adsorbate systems,[29–31] and etc., we employed the vdW correction proposed by Grimme (DFT + D3)[32,33] and implemented in VASP by Möllmann,[34] which yields better results than the previous Grimme's formulation called DFT + D2.[35]

In the DFT + D3 framework, the total energy $E_{\mathrm{DFT+D3}}$ is obtained by the sum of the self-consistent DFT total energy E_{DFT}, with the vdW correction E_{disp}, i.e.,

$$E_{\mathrm{DFT+D3}} = E_{\mathrm{DFT}} + E_{\mathrm{disp}}, \tag{1}$$

where E_{disp} is the sum of the two- and three-body energies, i.e., $E_{\mathrm{disp}} = E^{(2)} + E^{(3)}$, with

$$E^{(2)} = \sum_{AB} \sum_{n=6,8,10,\ldots} s_n \frac{C_n^{AB}}{r_{AB}^n} f_{d,n}(r_{AB}). \tag{2}$$

The first sum is over all atom pairs, while C_n^{AB} are the averaged nth-order dispersion coefficients ($n = 6,8,10,\ldots$) for the atom pairs AB.[33] r_{AB} is the internuclear distance and s_n is the scaling factor, which depends on the exchange-correlation (xc) functional, e.g., $s_n = 0.75$ for PBE. To avoid singularities for small interatomic distances r_{AB}, and double-counting effects of correlation at intermediate distances, a damping function $f_{d,n}$ is used, which controls the range of the dispersion interaction,[36] and it is given by

$$f_{d,n}(r_{AB}) = \frac{1}{1 + 6\left[r_{AB}/\left(s_{r,n} R_0^{AB}\right)\right]^{\alpha_n}}, \tag{3}$$

where $s_{r,n}$ is the order-dependent scaling factor of the cutoff radii. R_0^{AB} and α_n are adjusted parameters in such a way that the dispersion correction is less than 1% of the maximum E_{disp}. The three-body term is given by

$$E^{(3)} = \sum_{ABC} f_{d,(3)}\left(r_{ABC}^{\mathrm{av}}\right) E^{ABC}, \tag{4}$$

where the sum is over all atom triples ABC in the system. r_{ABC}^{av} is the averaged radius used as a damping function, and E^{ABC} is the nonadditive dispersion term from the third-order perturbation theory.[37,38] Further details can be found in Refs. 32 and 33. From now, DFT-PBE and DFT-PBE + D3 will be called shortly by PBE and PBE + D3, respectively.

The Kohn-Sham equations are solved with the projected augmented wave[39,40] (PAW) method, as implemented in VASP.[25,26] The equilibrium volume (lattice constants) and atomic positions of all crystal configurations of the PtX_2 (X = O, S, Se) compounds were obtained by minimizing the atomic forces and stress tensor using a plane-wave cutoff energy of 800 eV. For the Brillouin zone integration of the PtO_2 system in the $CaCl_2$-type structure, we employed a **k** mesh of $11\times11\times16$, and the same **k**-point density was used for all the remaining bulk calculations.

To obtain a better understanding of the role of the PBE + D3 functional (vdW corrections to the PBE functional) in the crystal structures of the PtO_2, PtS_2, and $PtSe_2$ compounds, we selected a set of trial crystal structures: (i) Experimentally reported x-ray diffraction (XRD) structures, i.e., CdI_2 type,[11] $CaCl_2$ type,[6–10] Rutile type[9,10] for PtO_2, CdI_2 type[12] for PtS_2, and CdI_2 type[11] for $PtSe_2$. (ii) Crystal structures selected among different oxides, e.g., the beta-tridymite, quartz, cristobalite, tridymite-ortho structures from the ZrO_2 and SiO_2 oxides, the anatase and Rutile from TiO_2, the $PbCl_2$ type from chlorides, and CaF_2 type from fluorides. All the selected crystal configurations are shown in Fig. 1 for the particular case of PtO_2.

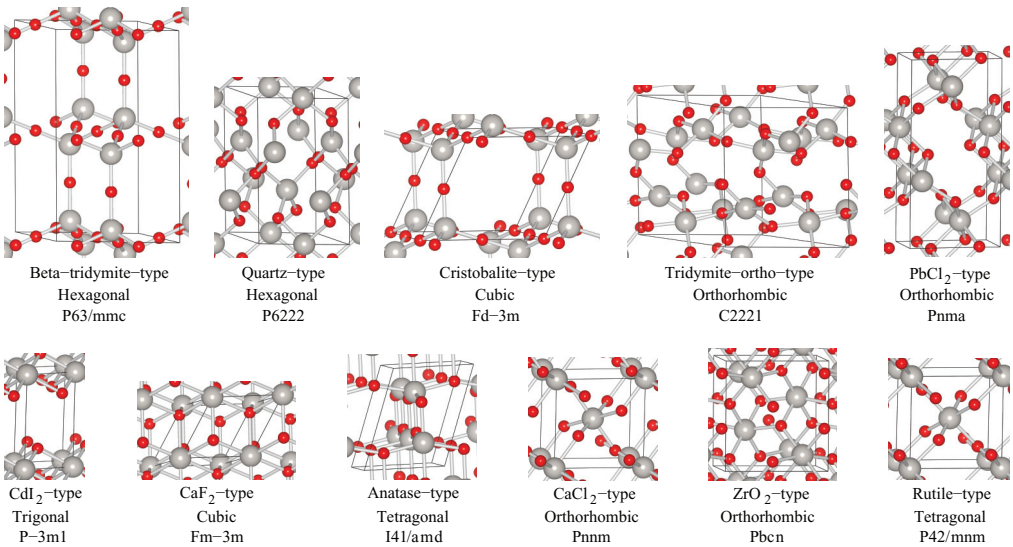

FIG. 1. (Color online) Crystal structures models employed for PtO_2 systems (the same set of structures have been employed for PtS_2 and $PtSe_2$ systems) [details in the Supplemental Material (Ref. 23)]. The Pt and O atoms are indicated by gray (large) and red (small) balls, respectively. The unit cells are indicated by continue black lines. The structure type, crystalline system, and space group are indicated below the unit cells.

TABLE I. Equilibrium lattice parameters (a_0, b_0, c_0), Pt–X (X = O, S, Se) bond lengths, and the relative total energies in relation to the CdI_2-type structure ΔE_{tot} for different configurations of the PtO_2, PtS_2, and $PtSe_2$ compounds.

Structure type	a_0 (Å)		b_0 (Å)		c_0 (Å)		Pt–X (Å)		ΔE_{tot} (eV)	
PtO_2	PBE	PBE + D3	PBE	PBE + D3	PBE	PBE + D3	PBE	PBE + D3	PBE	PBE + D3
Cristobalite	6.30	6.28	6.30	6.28	6.30	6.28	1.93	1.92	2.304	2.662
Beta-tridymite	6.21	6.16	6.21	6.16	10.54	10.61	1.93	1.92	2.289	2.645
Quartz	4.61	4.52	4.61	4.52	7.50	7.59	1.95	1.94	1.693	1.716
CaF_2	3.57	3.56	3.57	3.56	3.57	3.56	2.19	2.18	1.283	1.054
Tridymite-ortho	6.29	6.30	6.29	6.30	7.19	6.79	1.91	1.90	0.890	0.900
Anatase	4.02	3.98	4.02	3.98	5.67	5.61	2.04	2.03	0.721	0.704
CdI_2	3.15	3.16	3.15	3.16	4.93	4.02	2.05	2.04	0.000	0.000
Rutile	4.58	4.55	4.58	4.55	3.23	3.23	2.02	2.01	0.112	−0.097
$PbCl_2$	9.60	9.57	4.66	4.55	3.15	3.15	2.05	2.04	−0.002	−0.112
ZrO_2	5.22	5.21	4.54	4.50	5.60	5.59	2.03	2.02	0.079	−0.141
$CaCl_2$	4.59	4.56	4.55	4.53	3.18	3.17	2.03	2.02	−0.010	−0.227
PtS_2	PBE	PBE + D3	PBE	PBE + D3	PBE	PBE + D3	PBE	PBE + D3	PBE	PBE + D3
Cristobalite	7.35	7.33	7.35	7.33	7.35	7.33	2.25	2.24	2.658	3.290
Beta-tridymite	7.33	7.31	7.33	7.31	12.06	12.01	2.25	2.24	2.652	3.282
CaF_2	4.22	4.17	4.22	4.17	4.22	4.17	2.58	2.56	1.913	1.806
Anatase	4.71	4.67	4.71	4.67	6.82	6.75	2.41	2.39	1.199	1.331
Quartz	5.00	4.91	5.00	4.91	9.63	9.67	2.33	2.31	1.225	1.287
Rutile	5.45	5.36	5.45	5.36	3.82	3.82	2.40	2.38	1.050	0.964
ZrO_2	6.11	6.10	5.39	5.28	6.66	6.61	2.42	2.40	0.751	0.628
Tridymite-ortho	7.33	7.25	7.33	7.25	7.48	7.42	2.34	2.33	0.737	0.594
$CaCl_2$	5.34	5.26	5.53	5.47	3.70	3.70	2.42	2.40	0.719	0.587
$PbCl_2$	10.88	10.78	5.83	5.67	3.59	3.58	2.41	2.39	0.281	0.218
CdI_2	3.57	3.60	3.57	3.60	6.32	4.60	2.40	2.40	0.000	0.000
$PtSe_2$	PBE	PBE + D3	PBE	PBE + D3	PBE	PBE + D3	PBE	PBE + D3	PBE	PBE + D3
Beta-tridymite	7.84	7.81	7.84	7.81	12.75	12.73	2.40	2.39	2.835	3.628
Cristobalite	7.83	7.80	7.83	7.80	7.83	7.80	2.40	2.39	2.834	3.628
Quartz	5.73	5.59	5.73	5.59	9.36	9.49	2.44	2.42	1.453	1.774
CaF_2	4.45	4.40	4.45	4.40	4.45	4.40	2.72	2.69	1.479	1.507
Anatase	5.06	5.05	5.06	5.05	7.01	6.78	2.55	2.53	1.110	1.354
Rutile	5.78	5.69	5.78	5.69	4.02	4.02	2.54	2.51	1.010	1.069
Tridymite-ortho	7.76	7.67	7.76	7.67	8.03	7.94	2.47	2.45	0.690	0.638
ZrO_2	6.57	6.55	5.44	5.34	7.20	7.13	2.56	2.54	0.587	0.573
$CaCl_2$	5.48	5.37	5.99	5.94	3.91	3.90	2.56	2.55	0.558	0.536
$PbCl_2$	11.37	11.20	6.14	5.97	3.79	3.77	2.54	2.53	0.251	0.270
CdI_2	3.75	3.79	3.75	3.79	6.55	4.75	2.53	2.53	0.000	0.000

III. RESULTS

A. Relative total energies

The equilibrium lattice constants (a_0, b_0, c_0), the nearest neighbor distances (Pt–X), and the relative total energies per formula unit ($\Delta E_{tot} = E_{tot}^{trial} - E_{tot}^{CdI_2}$) are summarized in Table I for all structures and xc functionals. The atomic positions of the nonequivalent atoms for each crystal structure are reported in the Supplemental Material.[23] We found that both PBE and PBE + D3 functionals yield the same lowest energy structures for PtX_2, i.e., the distorted Rutile structure ($CaCl_2$ type) for PtO_2 and the CdI_2-type structure for both PtS_2 and $PtSe_2$ systems, however, we would like to mention that the vdW corrections affect the relative total energies, in particular, for PtO_2.

Among the 11 configurations calculated for PtO_2, we found that the lowest energy configurations (PBE and PBE + D3) are composed by a set of five nearly degenerated structures, namely, CdI_2 type, $CaCl_2$ type, Rutile type,[41] and the two structures ($PbCl_2$ type and ZrO_2 type) previously reported in Ref. 22. The maximum energy separation among the five lowest configurations is 0.122 eV (PBE) and 0.227 eV (PBE + D3), i.e., it depends on the functional. Although the lowest energy configuration is the same for both PBE and PBE + D3 functionals, there are changes in the relative energy differences. For example, the PBE energy difference among the layered CdI_2 and $CaCl_2$ structures is 0.010 eV, while it is 0.227 eV using PBE + D3, i.e., the vdW correction increases the energy difference. It is important to notice that the vdW correction does not favor layered structures in which the dispersion correction was expected to play an important role. Furthermore, we found that the vdW corrections increase the stability of the $PbCl_2$-type and ZrO_2-type structures.

In contrast with PtO_2, we found only two nearly degenerated structures for both dichalcogenides within the same relative energy range, which indicates a different behavior

compared with PtO_2. Both structures are the same using PBE or PBE + D3, Table I. The lowest energy structure obtained for PtS_2 and $PtSe_2$ is the CdI_2-type structure for both functionals, which is in excellent agreement with previous results.[11,42,43] The relative energy differences between the first and the second lowest energy structures for PtS_2 and $PtSe_2$ are 0.281 eV/f.u. (0.218 eV/f.u.) and 0.251 eV/f.u. (0.270 eV/f.u.), respectively, for PBE (PBE + D3), which confirms the high stability of layered CdI_2-type structure for platinum dichalcogenides. Furthermore, from Table I we can see a similar stability order for PtS_2 and $PtSe_2$, using PBE and PBE + D3, except for the PtS_2 anatase-type and quartz-type structures and $PtSe_2$ quartz-type and CaF_2-type structures.

B. Equilibrium lattice constants

In the five lowest energy PBE and PBE + D3 configurations for PtO_2, the Pt and O atoms form almost perfect octahedron motifs, i.e., the Pt atoms are surrounded by six O atoms. The Pt–O distances are 2.02–2.05 Å (PBE), while the PBE + D3 Pt–O distances are 0.5% smaller than the PBE results. Thus, the vdW correction almost does not affect the Pt–O bond. The $PbCl_2$ structure is characterized by the presence of large empty spaces (called holes in this work), which contract by about 0.3% and 2.4% along of the a_0 and b_0 directions, respectively, due to the vdW corrections. The CdI_2 structure is formed by the stacking of PtO_2 layers, for which $c_0 = 4.93$ Å (PBE) and 4.02 Å (PBE + D3), i.e., a contraction of 18.5% upon the addition of the vdW correction to the PBE functional. Thus, these results indicate clearly that the interaction between the layers is dominated by nonlocal vdW interactions. However, we would like to point out that a better description of the CdI_2 structure does not necessarily imply an increasing in the energetic stability, as discussed above.

In the lowest energy PtS_2 and $PtSe_2$ structures, the S and Se atoms form octahedron motifs with the Pt atoms, except for the Trydimite-ortho-type structure, where the Pt atoms are surrounded by 4 O atoms, i.e., forming planes. The Pt–S and Pt–Se distances are in the range 2.34–2.42 Å (PBE) for PtS_2 and from 2.47 to 2.56 Å for $PtSe_2$, which the PBE + D3 functional reduces the bond lengths by about 0.4% and 0.8%, respectively. The bond Pt–S and Pt–Se lengths are larger than the Pt–O, which is expected based on the atomic radius of the S and Se species.[44]

We found that the vdW corrections improve the agreement with the experimental results, in particular, for the CdI_2-type structure, which is among the five lowest energy structures for PtO_2, and the lowest energy structure for PtS_2 and $PtSe_2$. Furthermore, we observed improvements even for the lowest energy $CaCl_2$-type structure for PtO_2, e.g., the experimental lattice parameters are $a_0 = 4.48, b_0 = 4.54$, and $c_0 = 3.14$ Å,[45] while the PBE (PBE + D3) results differ by +2.5% (+1.8%), +0.2% (−0.2%), +1.3% (+0.9%), respectively. For PtS_2 and $PtSe_2$ in the CdI_2-type structure, the experimental lattice constants are $a_0 = 3.54, c_0 = 5.04$ Å, and $a_0 = 3.73, c_0 = 5.08$ Å,[11] respectively, while the PBE results are overestimated by 0.8%, 25.4%, and 0.5%, 28.9%, respectively. The PBE + D3 results deviates by +1.7%, −8.7%, and +1.6%, −6.5% for PtS_2 and $PtSe_2$, respectively.

We noticed that PBE strongly overestimates c_0 in the CdI_2-type structure, which is expected as PBE does not provide a reliable description of weak interacting vdW systems, i.e., in general PBE overestimates the equilibrium distances of weak interacting systems.[15,17–19] Furthermore, we found that PBE + D3 underestimates the lattice c_0 constant by a substantial value, i.e., about 6%–8%, which indicates that the parameters employed in the DFT + D3 framework might overestimate the strength of the vdW correction. Although the DFT + D3 formulation is very simple, it relies heavily on the calculation of the C_6^{AB} parameters from molecular systems, which directly determines the quality of the results.

C. Interlayer spacing

To obtain a better understanding of the role of the vdW corrections for the CdI_2-type structure for the PtX_2 compounds, we calculated the total energy as a function of the interlayer separation. For each layer separation, a_0 was set up to the equilibrium value and the atomic positions of the atoms were optimized. The interlayer interacting for the PtO_2, PtS_2, and $PtSe_2$ systems are shown in Fig. 2. Employing the PBE functional, we obtained an interacting energy among the layers of 2 meV for PtO_2, 5 meV for PtS_2, and 6 meV for $PtSe_2$, while for the PBE + D3 functional, we obtained 310, 380, and 490 meV, respectively. Thus, the vdW correction plays an important role in improving the description of the CdI_2 structure, however, as mentioned above, it does not increase the relative stability of the CdI_2 structure compared with other trial structures.

Björkman *et al.*[28] has simulated exfoliation for a series of multilayer systems by peeling off the top layer and the difference between interlayer binding energy and exfoliation energy is smaller than 4%, because of surface relaxation effects, and hence, the interlayer binding energy is related to the exfoliation energy. For the CdI_2-type compounds, we found 310, 380, and 490 meV for PtO_2, PtS_2, and $PtSe_2$, respectively. Thus, the exfoliation energy is larger for the $PtSe_2$ system, while it is smaller for PtO_2.

D. Electronic structure

Among the 11 studied configurations, we selected five crystal structures, namely, CdI_2, Rutile, $PbCl_2$, ZrO_2, and $CaCl_2$, for the analysis of the vdW corrections in the total density of states (TDOS), which are shown in Fig. 3 for the PtO_2, PtS_2, and $PtSe_2$ compounds and PBE and PBE + D3 functionals. The differences in the PBE and PBE + D3 TDOS are indirect changes due to the changes in the equilibrium volume, which affects the electron density, and hence, the electronic states. The PBE and PBE + D3 functionals yields nearly the same TDOS for all compounds and structures, except for PtS_2 and $PtSe_2$ in the CdI_2 structure. For example, for CdI_2, the PBE functional yields an energy band gap of 1.37 and 0.78 eV for PtS_2 and $PtSe_2$, respectively, however, the addition of the nonlocal vdW correction to the PBE functional turns the systems into metals, while the bottom of the valence band shifts down.

In contrast, there is almost no difference in the PBE and PBE + D3 TDOS for PtO_2 in the CdI_2 structure, which can be

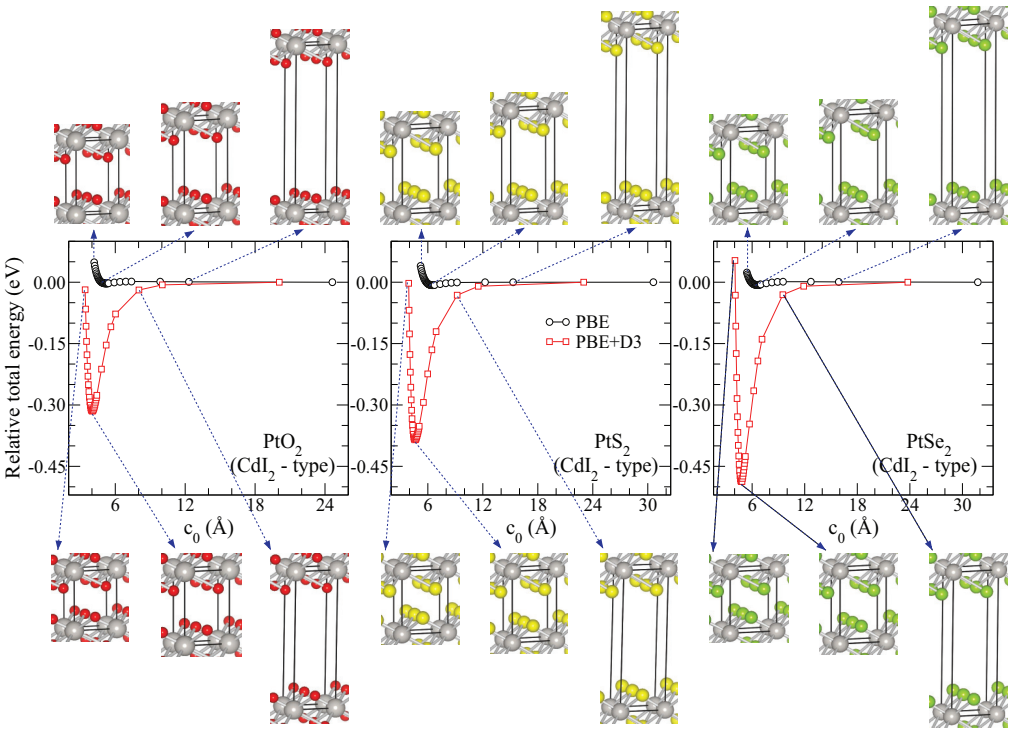

FIG. 2. (Color online) Relative total energy as function of the c_0 parameter for PtO_2, PtS_2, and $PtSe_2$ in the CdI_2-type structure. The black (circles) and red (squares) lines are the calculated CdI_2-type configurations for PBE and PBE + D3, respectively.

explained as follows. For PtO_2, we found a contraction in the lattice parameter c_0 upon the vdW correction of about 18%, while for the PtS_2 and $PtSe_2$ systems in the same structure, the contraction of the lattice parameter c_0 is about 27% upon the vdW correction, i.e., substantially larger than for PtO_2 in the CdI_2 structure. The changes in the TDOS can be also correlated

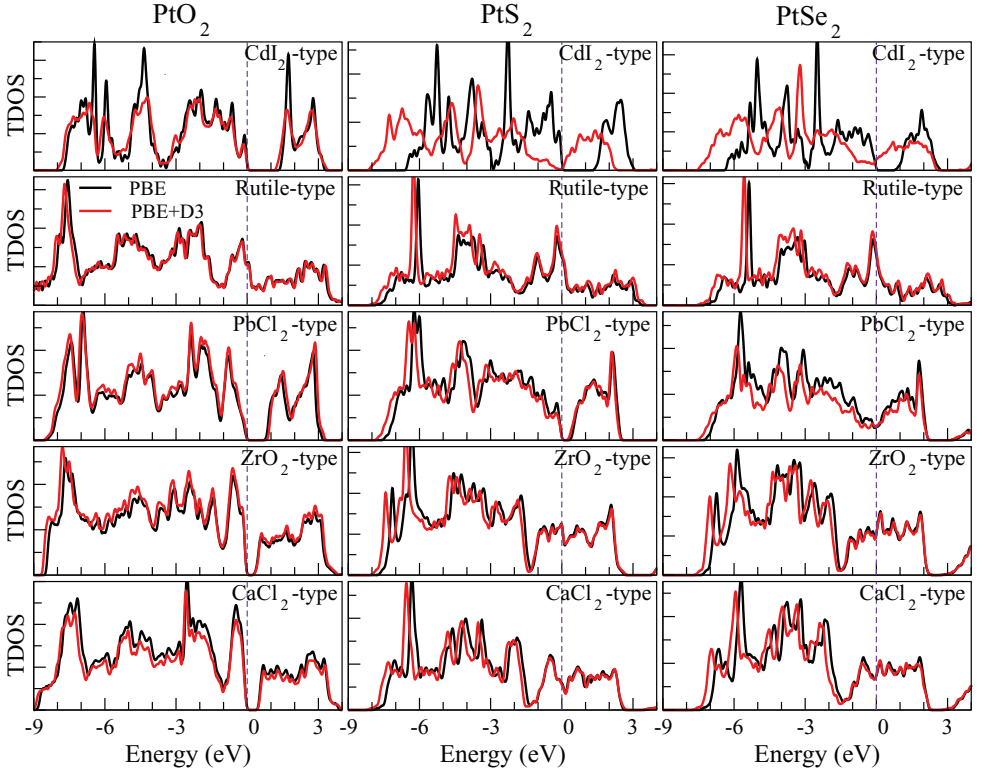

FIG. 3. (Color online) Total density of states (TDOS) for the five lowest energy PtO_2 structures in arbitrary units in the first column and the TDOS for the same structures for PtS_2 (second column) and $PtSe_2$ (third column) compounds. The black and red lines are the TDOS for PBE and PBE + D3 calculations, respectively. The vertical dashed lines indicate the Fermi level (zero energy).

with the magnitude of the interlayer binding energy, which is smaller for PtO_2 and larger for PtS_2 and $PtSe_2$, see Fig. 2.

Previous results[27,42] have suggested a semiconductor character for PtS_2 in the CdI_2 structure with an energy band separating the *d*-band manifold. This result is consistent with the PBE results, however, the addition of the vdW correction to the PBE functional yields a contraction of 27% of c_0, which in turns strongly affects the band gap, however, we mentioned above that the equilibrium PBE + D3 lattice constant is about 7% smaller than the experimental, and hence, it affects the value of the energy band gap. For $PtSe_2$, the experimental studies have reported a semiconductor state[46] and a semimetal state,[27,42,47] which shows similar problem as discussed for PtS_2, i.e., a strong overestimation of the lattice parameter c_0 affects directly the comparison between experimental and theoretical results.

IV. SUMMARY

In this work we investigated the role of the vdW corrections added to the PBE functional (PBE + D3) in the structural, energetics, and electronic properties of the PtX_2 (X = O, S, Se) compounds. We found that the PBE and PBE + D3 functionals yield the same lowest energy configuration for the PtO_2, PtS_2, and $PtSe_2$ compounds, i.e., $CaCl_2$ for PtO_2 (in agreement with previous DFT calculations[21,22]), and CdI_2 for PtS_2 and $PtSe_2$ (which is consistent with experimental observations[11,12]). However, we found that the PBE + D3 functional changes the relative total energy among the configurations compared with PBE results, in particular, for the PtO_2 system. As expected, we found that the vdW correction plays a fundamental role in the equilibrium volume of the CdI_2 structure, i.e., it compresses the lattice parameter c_0 compared with experimental results. Furthermore, PBE + D3 decreases the relative error compared with experimental results from about +27% (PBE) to about −7%, however, it does not increase the stability of the CdI_2 structure compared with other systems for which the vdW correction does not play a major role. Due to the indirect effects (volume compression), we found that the density of states of the PtS_2 and $PtSe_2$ in the ground state structure is strongly affected the vdW correction, which is overestimated due to the underestimation of the equilibrium volume.

ACKNOWLEDGMENTS

We are grateful for the financial support of the São Paulo Science Foundation (FAPESP). The infrastructure provided to our computer cluster by the Centro de Informática de São Carlos (Universidade de São Paulo) is acknowledged. The authors thank Dr. Stefan Grimme and Jonas Möllmann for providing the D3 subroutines to be added in VASP.

*mauriciomjp@gmail.com
†ricardo.nomiyama@gmail.com
‡Corresponding author: juarez_dasilva@iqsc.usp.br

[1] N. Sabourault, G. Mignani, A. Wagner, and C. Mioskowski, Organic Lett. **4**, 2117 (2002).
[2] S. Dey and V. K. Jain, Platinum Metals Rev. **48**, 16 (2004).
[3] X.-Q. Gong, R. Raval, and P. Hu, Phys. Rev. Lett. **93**, 106104 (2004).
[4] M. D. Ackermann, T. N. Pedersen, B. L. N. Hendriksen, O. Robach, S. C. Bobaru, I. Popa, C. Quiros, H. Kim, B. Hammer, S. Ferrer *et al.*, Phys. Rev. Lett. **95**, 255505 (2005).
[5] F. Parsapour, D. F. Kelley, and R. S. Williams, J. Phys. Chem. B **102**, 7971 (1998).
[6] O. Muller and R. Roy, J. Less-Common Met. **16**, 129 (1968).
[7] M. Salmerón, L. Brewer, and G. A. Somorjai, Surf. Sci. **112**, 207 (1981).
[8] A. N. Mansour, D. E. Sayers, J. W. Cook, Jr., D. R. Short, R. D. Shannon, and J. R. Katzer, J. Phys. Chem. **88**, 1778 (1984).
[9] M. P. H. Fernandez and B. L. Chamberland, J. Less-Common Met. **99**, 99 (1984).
[10] Y. Abe, M. Kawamura, and K. Sasaki, Jpn. J. Appl. Phys. **38**, 2092 (1999).
[11] S. Furuseth, K. Selte, and A. Kjekshus, Acta Chem. Scand. **19**, 257 (1965).
[12] A. Finley, D. Schleich, J. Ackerman, S. Soled, and A. Wold, Mat. Res. Bull. **9**, 1655 (1974).
[13] S. Grimme, Wiley Interdiscip. Rev. Comput. Mol. Sci. **1**, 211 (2011).
[14] J. Klimeš and A. Michaelides, J. Chem. Phys. **137**, 120901 (2012).
[15] H. Rydberg, M. Dion, N. Jacobson, E. Schröder, P. Hyldgaard, S. I. Simak, D. C. Langreth, and B. I. Lundqvist, Phys. Rev. Lett. **91**, 126402 (2003).
[16] M. Hasegawa and K. Nishidate, Phys. Rev. B **70**, 205431 (2004).
[17] A. N. Kolmogorov and V. H. Crespi, Phys. Rev. B **71**, 235415 (2005).
[18] N. Ooi, A. Rairkar, L. Lindsley, and J. B. Adams, J. Phys.: Condens. Matter **18**, 97 (2006).
[19] J. L. F. Da Silva and C. Stampfl, Phys. Rev. B **76**, 085301 (2007).
[20] G. Graziano, J. Klimes, F. Fernandez-Alonso, and A. Michaelides, J. Phys.: Condens. Matter **24**, 424216 (2012).
[21] N. Seriani, Z. Jin, W. Pompe, and L. Colombi Ciacchi, Phys. Rev. B **76**, 155421 (2007).
[22] R. K. Nomiyama, M. J. Piotrowski, and J. L. F. Da Silva, Phys. Rev. B **84**, 100101(R) (2011).
[23] See Supplemental Material at http://link.aps.org/supplemental/10.1103/PhysRevB.88.075421 for PtO_2, PtS_2, and $PtSe_2$ atomic positions of the nonequivalent atoms for each crystal structure.
[24] J. P. Perdew, K. Burke, and M. Ernzerhof, Phys. Rev. Lett. **77**, 3865 (1996).
[25] G. Kresse and J. Hafner, Phys. Rev. B **48**, 13115 (1993).
[26] G. Kresse and J. Furthmüller, Phys. Rev. B **54**, 11169 (1996).
[27] D. Dai, H.-J. Koo, M.-H. Whangbo, C. Soulard, X. Rocquefelte, and S. Jobic, J. Solid State Chem. **173**, 114 (2003).
[28] T. Björkman, A. Gulans, A. V. Krasheninnikov, and R. M. Nieminen, Phys. Rev. Lett. **108**, 235502 (2012).
[29] J. L. F. Da Silva, C. Stampfl, and M. Scheffler, Phys. Rev. Lett. **90**, 066104 (2003).
[30] J. L. F. Da Silva, C. Stampfl, and M. Scheffler, Phys. Rev. B **72**, 075424 (2005).

[31]W. Liu, J. Carrasco, B. Santra, A. Michaelides, M. Scheffler, and A. Tkatchenko, Phys. Rev. B **86**, 245405 (2012).
[32]S. Grimme, J. Comp. Chem. **27**, 1787 (2006).
[33]S. Grimme, J. Antony, S. Ehrlich, and H. Krieg, J. Chem. Phys. **132**, 154104 (2010).
[34]J. Möllmann (private communication).
[35]T. Bučko, J. Hafner, S. Lèbegue, and J. G. Ángyán, J. Phys. Chem. A **114**, 11814 (2010).
[36]J.-D. Chai and M. Head-Gordon, Phys. Chem. Chem. Phys. **10**, 6615 (2008).
[37]B. M. Axilrod and E. Teller, J. Chem. Phys. **11**, 299 (1943).
[38]Y. Muto, Proc. Phys. Math. Soc. Jpn. **17**, 629 (1943).
[39]P. E. Blöchl, Phys. Rev. B **50**, 17953 (1994).
[40]G. Kresse and D. Joubert, Phys. Rev. B **59**, 1758 (1999).
[41]S. Zhuo and K. Sohlberg, Physica B **381**, 12 (2006).
[42]S. Soled, A. Wold, and O. Gorochov, Mat. Res. Bull. **11**, 927 (1976).
[43]G. Y. Guo and W. Y. Liang, J. Phys. C: Solid State Phys. **19**, 995 (1986).
[44]C. Kittel, *Introduction to Solid State Physics*, 7th ed. (John Wiley and Sons, New York, 1996).
[45]K.-J. Range, F. Rau, and A. M. Heyns, Mater. Res. Bull. **12**, 1541 (1987).
[46]F. Hulliger, J. Phys. Chem. Solids **26**, 639 (1965).
[47]G. Kliche, J. Solid State Chem. **56**, 26 (1985).